AIMS Bioengineering

AIMS Bioengineering, 8(1): 95–111.
DOI: 10.3934/bioeng.2021010
Received: 30 October 2020
Accepted: 31 December 2020
Published: 21 January 2021

http://www.aimspress.com/journal/Bioengineering

Research article

Influence of plantation climate and storage time on thermal and viscoelastic properties of natural rubber

Allen Jonathan Román[1,*], Jamelah Zena Travis[2], Juan Carlos Martínez Ávila[3] and Tim A. Osswald[1]

[1] Polymer Engineering Center, Department of Mechanical Engineering, University of Wisconsin, Madison, WI, USA
[2] General Motors Global Technical Center, GMNA, Detroit, MI, USA
[3] Colombo Argentina Natural Rubber Society, Bogotá, Colombia

* **Correspondence:** Email: ajroman@wisc.edu; Tel: +12629605660.

Abstract: The Sociedad de Caucho Colombo Argentina (SOCCA) collected natural rubber (NR) from Yarima, Colombia, for seven months spanning two years. The unvulcanized NR was used to conduct a preliminary study, part of a long-term study, to uncover some underlying mechanisms in charge of imparting variation between NR batches, such as the collection site's rainfall conditions and storage period by using calorimetry, rheometry, and a dynamic mechanical analyzer. The ultrasound study found that an increase in monthly rainfall increased the material's elastic constant at 10 MHz, and the crystallization study uncovered that the amount of crystallization decreased with increased rain while remaining relatively constant if rainfall was within the recommended rainfall amount for the tree. Additionally, stress relaxation measurements revealed that an increase in rainfall suggested an increase in the material's temperature sensitivity. The temperature sensitivity relates to the material's processability in which an increase in temperature with high sensitivity will have a more drastic decrease in stress during a relaxation test compared to a material with low sensitivity.

Keywords: natural rubber; rainfall; aging; rubber production

Abbreviations: Natural Rubber (NR); Proton Nuclear Magnetic Resonance (^{1}H-NMR); Dynamic Mechanical Analyzer (DMA); Differential Scanning Calorimetry (DSC); Thermogravimetric analysis (TGA)

1. Introduction

In this study, *non vulcanized* natural rubber obtained from the *Hevea brasiliensis* tree in Yarima, Colombia, underwent thermal and viscoelastic characterization to provide some of the differences in properties amongst NR produced in various months to highlight some climate-induced changes to the material and storage-induced material behavior. Climate plays a significant role in agriculture regarding yield and quality as it influences the soil's chemistry and physical characteristics. In relation, rainfall is a dominating factor in tropical agriculture as it is the primary source of moisture available in the soil, which is made available to the plants. Umar et al. conducted a 31-year study where the results revealed that rainfall, minimum and maximum temperature, as well as the age of the rubber tree, had a positive coefficient of correlation on latex yield [1]; therefore, the variability in rainfall throughout the year can be a crucial factor over the production and properties in NR.

Research has indicated that the optimal climatic conditions require 160 to 275 millimeters of monthly rainfall with no severe dry season to produce latex consistently. This amounts to 125–150 annual rain days, and evenly distributed rainfall of 1800–2000 mm on well-drained soil is best [2]. It has also been discovered that heavy rainfall can significantly reduce harvesting concentrations, decreasing the number of tapping days per year due to a reduction in tapping intensity of latex yields [3,4].

These characteristic changes in material properties bring insight into how plantations can improve their material quality by standardizing their collection and irrigation procedures to provide the industry with consistent quality.

Today, one of the manufacturing industry's primary thrusts has been investigating alternative, eco-friendly product design materials. As technology evolves, so do the adverse effects it has on our ecosystems since increasingly high consumer industries' demands have increased the number of toxic chemicals entering natural environments. Among these sustainable materials, natural rubber (NR) has been of piquing interest for composite materials because of its low cost, nontoxicity, and excellent physical properties [5]. Seeking materials with high strength and compliance characteristics has led scientists to develop polymer composites that combine a high strength material with a material that can withstand large deformations as the curled polymer chains can stretch well above 400% elongation [6,7]. Because of these characteristics, rubber is used in numerous products within the automotive industry, orthopedics, construction, and food storage. However, the material properties of NR components change depending on the storage time, production climate, processing conditions of the latex, and material handling post-processing [3,8,9,10]. Therefore, NR material is subject to chemical changes due to many variables, such as aging and storage time. Additionally, due to the polymer molecule's unstable nature, NR molecules degrade, causing the material to depolymerize and possibly lose some performance characteristics.

The chemical name for NR is polyisoprene; the isoprene monomer polymerizes after being extracted from the tree. Polyisoprenes have a total of four different isomers in their polymer chain: *cis*-1,4, *trans*-1,4:1,2:3,4. However, natural rubber is known to have the main chain structure consisting almost entirely of the *cis*-1,4 polyisoprene [11]. The exclusive *cis*-geometry surrounding the C=C bonds is responsible for NR's specific properties, making the polymer stereoregular [12], a crucial factor of NR as it accounts for the desirable properties and mechanical strength. Unfortunately, stereoregularity is also responsible for NR's crystallization upon storage at room temperature [13,14], and having high yields of *cis*-1,4 usually lowers the glass transition temperature,

which increases crystallinity to improve mechanical strength.

It has been determined that the naturally occurring NR molecule contains around 90–98% *cis*-1,4 polyisoprene units, where two or three *trans*-1,4 units are found at the terminal ends of the polymer chain resulting from the initiating reaction during the rubber biosynthesis process [15,16,17]. Moreover, it was essential to determine that the rubber plantation materials in Yarima, Colombia, were primarily made up of larger amounts of *cis*-1,4 polyisoprene to conduct the characterization experiments. A high- resolution ^{1}H-NMR spectroscopy experiment of the NR material produced in other months was conducted in $CDCl_3$ solution. The protons are labeled as follows:

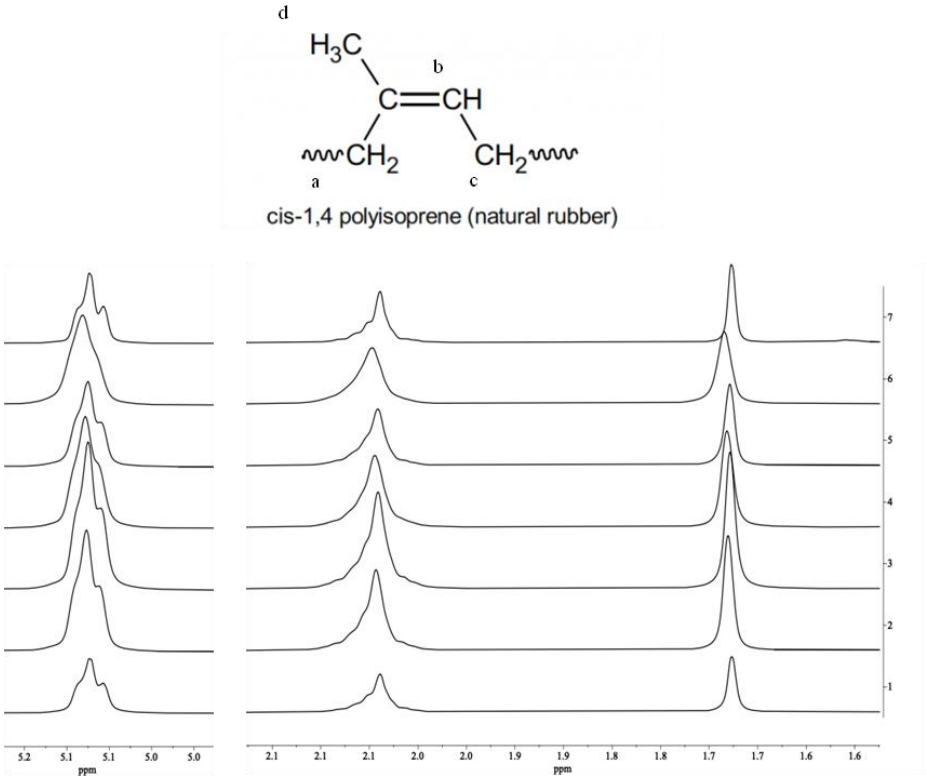

Figure 1. ^{1}H-NMR spectra of *cis*-1,4 polyisoprene measured in $CDCl_3$ for rolls corresponding to October 2017(1), November 2017(2), December 2017(3), June 2018(4), July 2018(5), August 2018(6), and September 2018(7).

As mentioned above, the three signals for the *cis*-1,4 polyisoprene were assigned to the olefinic proton (H_b), the methylene protons (H_a and H_c), and the methyl proton (H_d) [18]. In all NR sample cases, *cis*-1,4 polyisoprene exhibited signals around 5.0 ppm, 2.0 ppm, and 1.68 ppm to the assigned protons seen in Figure 1, and the signal for *trans*-1,4 polyisoprene (1.6 ppm) was not *significantly* detected in this study [19]. This data determined that the obtained NR samples were *primarily* made up of *cis*-1,4 polyisoprene units. Since this study is not centered around the exact structure and composition of the natural rubber samples, a higher resolution NMR spectroscopy experiment was not performed. As mentioned, it is recognized that the NR samples contain some amount of the *trans*-1,4 confirmation; however, according to Figure 1, this confirmation was not significantly signaled.

2. Materials and methods

2.1. NR collection

SOCCA provided the Polymer Engineering Center at the University of Wisconsin Madison with FX 3864 clone NR roll samples collected on October, November, and December from 2017 and June, July, August, September from the year 2018.

2.2. DSC measurements

DSC measurements were conducted on the Netzsch DSC214 Polyma instrument. A cooling unit allowed measurements to reach a minimum temperature of −40 °C while employing nitrogen as the purge gas. NR is a minimally unstable material where additional crystallization during storage and loading can occur [20]. 5 ± 0.5 mg NR samples were encapsulated in a standard aluminum pan along with its pierced lid and were heated to 120 °C at 5 °C/min, and then held for 5 minutes to ensure an isothermal state to erase the thermal history of the sample before experimentation. Once the isothermal step was complete, the sample was quench cooled to −23 °C at 40 °C/min and held in a hermetically sealed container for 2 h to ensure the sample reached constant temperature throughout the natural rubber specimen without moisture absorption. The heat of fusion experiments was then conducted by taking the sample and heating it to 200 °C at 100 °C/min, and the endothermic peak onsets and area of the peak of each experiment were determined with the Netzsch Proteus Software. Five samples from each roll were characterized to confirm the absence of variation within the roll and repeatability of experiments.

2.3. TGA measurements

All thermogravimetric measurements were made using the Netzsch TG209 F1 Libra equipped with a heating unit capable of reaching 1100 °C from room temperature in a nitrogen or air atmosphere. 10 ± 1 mg natural rubber samples in a ceramic crucible were heated to 600 °C at 10 °C/min, and the sample mass was logged with respect to time and temperature with an optimal resolution of 0.01 μg.

2.4. Ultrasound

The Panametrics Model 500 PR was utilized as the ultrasonic transmitter and receiver, while 10 MHz longitudinal wave transducers (Panametrics Model V110) were used in conjunction with the Tektronix DPO 3014 digital phosphor oscilloscope to send and read signals. Natural rubber samples were compressed to a 2 mm thickness with a larger diameter than the transducers. The samples were placed between both transducers while employing water as the coupling agent. Once placed within both transducers, the time delay between the sent pulse and the received pulse was logged with the oscilloscope. Knowing the sample geometry allowed for the calculation of the signal speed. This signal speed was translated to an elastic constant via Eq 1 below, where c_L is the longitudinal wave speed and ρ is the material density [21]. One sample from each corner of the roll was characterized in this non-destructive mechanical test, and no variation within the roll was captured.

$$c_L = \sqrt{\frac{C_{1111}}{\rho}} \tag{1}$$

2.5. Parallel plate rheometer

The advanced rheometric expansion system TA instruments ARES was used to conduct stress relaxation measurements. This instrument can subject the sample to either a dynamic or steady shear strain deformation. With the appropriate cooling system, the system has a working temperature range of −150 to 600 °C and a transducer torque range of 0.2 to 100 μN/m. Additionally, the rheometer can be used as a parallel plate rheometer or a cone and plate rheometer of varying plate geometries.

Stress relaxation measurements were conducted by imposing a steady shear strain deformation of γ = 10% at 210 °C and 250 °C to understand how high processing temperatures can alter the NR's viscoelastic behavior. Five repetitions were conducted to ensure repeatability and to confirm that there is no variation within each unique NR roll. While deformed, the natural rubber sample's stress was measured and logged with respect to time. In theory, the time required for the sample to reach 1% of the max shear stress is categorized as the stress relaxation time. In this study, five percent of the maximum stress was selected as the relaxation cut off point to minimize the amount of noise-induced by reaching a low-resolution region of the instrument, as 1% fell within the data acquisition's lower limits system's capabilities.

2.6. Dynamic mechanical analyzer

The Netzsch Explexor 500 Newton Dynamic Mechanical Analyzer (DMA) was used to conduct stress relaxation measurements in tension. Netzsch's DMA has a working temperature ranging from 21 to 1500 °C with a maximum load capacity of 500 Newtons. NR Samples were heated similarly to the ultrasound sample to erase any load-induced crystallization and thermal history. The heated samples were then compressed to a thickness of 3 mm, and once flattened, the samples were removed from the compression fixture, and rectangular samples were cut out to a width of 10 mm.

Stress relaxation measurements in tension were conducted on the rectangular NR sample where the sample experienced a steady tensile strain of 10%, 30%, and 50%, at 21 °C, 50 °C, and 80 °C to understand the temperature-dependent viscoelastic behavior of NR. Samples were cut from all four corners to check for variability within the roll while having 3 repetitions per location to ensure repeatability. Variability within the roll was not observed, and being as it takes hours for NR to experience 1% of the maximum stress in solid-state, a characteristic relaxation time was chosen in being the time it takes for NR to experience 65% of the maximum stress.

2.7. High-Resolution ^{1}H-NMR Spectroscopy

The Bruker Avance—400 proton nuclear magnetic resonance spectrometer was used to perform proton NMR spectroscopy on each of the NR samples. The specific Bruker Avance used features a 400 MHz, 2-channel spectrometer with Z-gradient equipped for gradient shimming, a standard BBFO Z-gradient SmartProbe with an automatic tune and match, and a 1H direct- and indirect-detection of heteronuclei was used. The magnet core was cooled to a very low temperature using liquid nitrogen and helium to maintain a superconducting system. The shim system was held at

room temperature and was mounted to the lower end of the magnet to maximize the field homogeneity [22].

The samples were prepared by cutting small pieces of each corner of the NR rolls from all months. Each corner was prepared and analyzed. For each NMR sample, 5–25 mg of the cut pieces were added to the bottom individual NMR tubes and dissolved in approximately 1 mL of deuterated carbon tetrachloride ($CDCl_3$) solution with tetramethylsilane (TMS) as the internal standard. Signals for TMS (δH 0 ppm) were used for chemical shift referencing. Since the degree of separation of the two peaks corresponding to *cis*-1,4 and *trans*-1,4 is solvent dependent due to the slight differences in how the solvent affects the methyl groups, $CDCl_3$ was the solvent of choice because of its great separation between the two peaks [23].

3. Results and discussion

3.1. Rainfall

Weather stations on the plantation collected rainfall data, which were used to compare to the differential scanning calorimetry studies and dynamic mechanical tests conducted on each respective month's material. NR rolls from each distinct month were received from SOCCA, and Figure 2 depicts the rainfall data for each respective month.

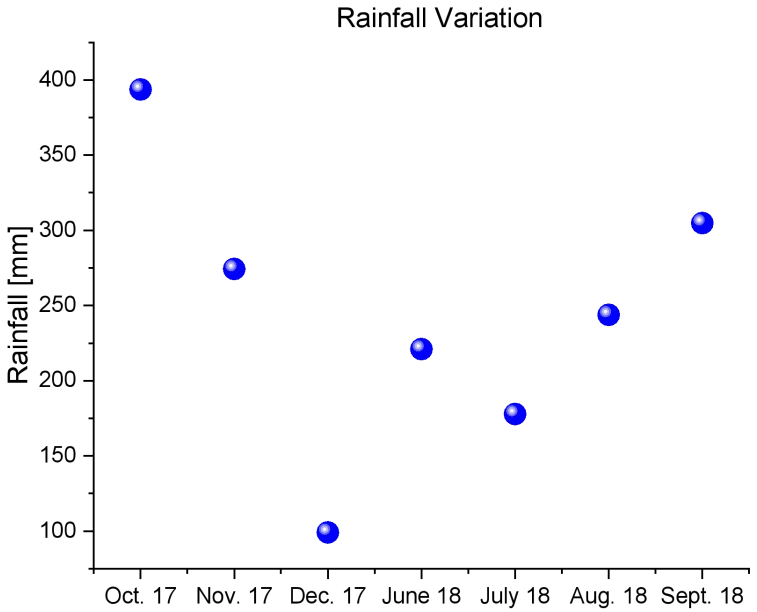

Figure 2. Rainfall amount variation by month and year in Yarima, Columbia.

3.2. Differential scanning calorimetry studies

Quantifying the area under the DSC curve gives us an indirect measurement of crystallization within the NR sample. As mentioned, NR crystallizes when strained and during storage time [24]. The area under the curve is referred to as the heat of fusion, also known as the absorbed energy, and

can be seen to fluctuate over time depending on the collection date. The amount of crystallization present in rubber impacts the thermal properties, the mechanical and viscoelastic response of the material; therefore, consistent heat of fusion is desired as it would reduce variability in material properties between batches. The variation in the heat of fusion between collection dates can be seen in Figure 3 below, where the gray region represents the optimal amount of rain required by the tree to survive, dictated by Rao and Vijayakumar. Noting that the left y-axis of Figure 3 has the large value at the bottom of the axis and the smallest on top, samples collected from the year 2017 demonstrate that a decrease in rainfall translates to an increase in the heat of fusion, and if near the recommended rainfall zone, such as June, July, August, and September of 2018, then the amount of crystallization is more consistent throughout the respective month. The flipped y-axis served as a method to visualize the following trend and the phenomena of material crystallization variation due to rainfall.

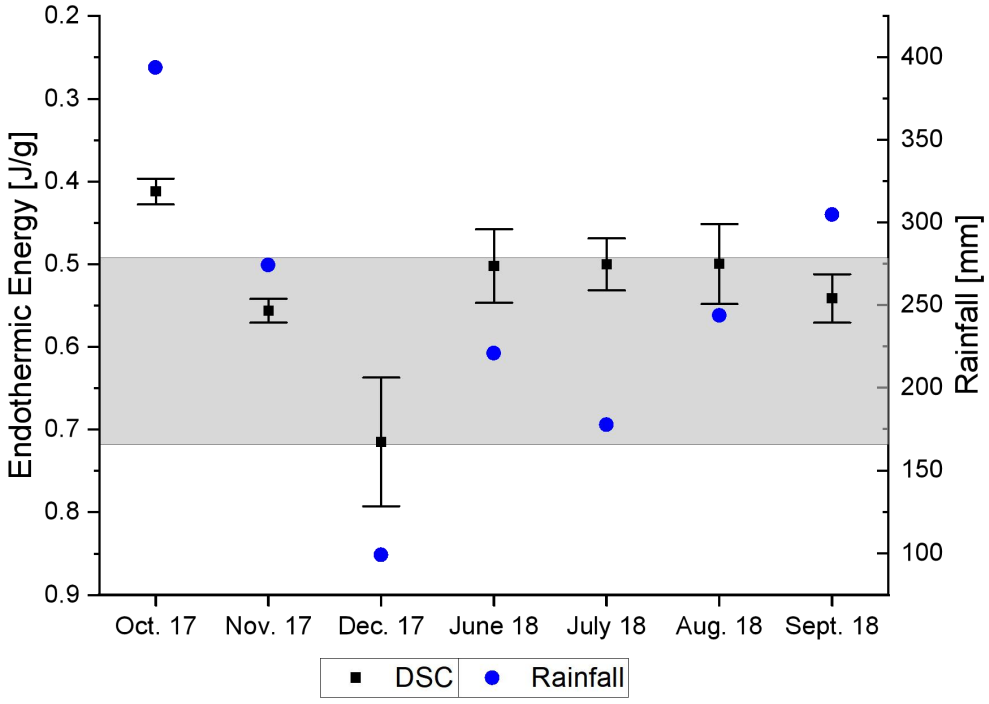

Figure 3. Graph showing the heat of fusion variation amongst NR extraction dates where the error bars represent ±1 standard deviation from the mean. The gray region represents the maximum and minimum amount of rainfall required by the tree.

During dry periods, the tree experiences low turgor pressure, which translates to a relatively smaller pressure exerted on the latex vessels in charge of secretion. A tree functioning on relatively low turgor pressure results in differences in the percent in latex total solids referred to as the dilution index [25].

Additionally, outdoor temperature, wind speed, gust speed, and wind chill data were collected from the weather station, but no correlation was determined with those climate conditions with DSC experiments. For example, October through December shows a decreasing DSC output trend, which

does not agree with outdoor temperature trends where the average monthly temperatures for those three months are 26.4 °C, 23.9 °C, and 28.2 °C, respectively. Furthermore, SOCCA can continue monitoring the climate at the plantation while producing NR, and it would be beneficial to continue this study through the upcoming years to solidify the understanding of climate-induced crystallization of NR.

3.3. Resonant ultrasound studies

NR samples were kept at 80 °C for an hour to dry and erase the material's thermal history. The samples were then subject to ultrasound testing to determine the time needed for the ultrasound wave to travel from the transducer, through the material, and onto the receiver. A depiction of the experimental setup can be seen below in Figure 4, where the yellow cylindrical piece between the transducer and the receiver is the NR sample.

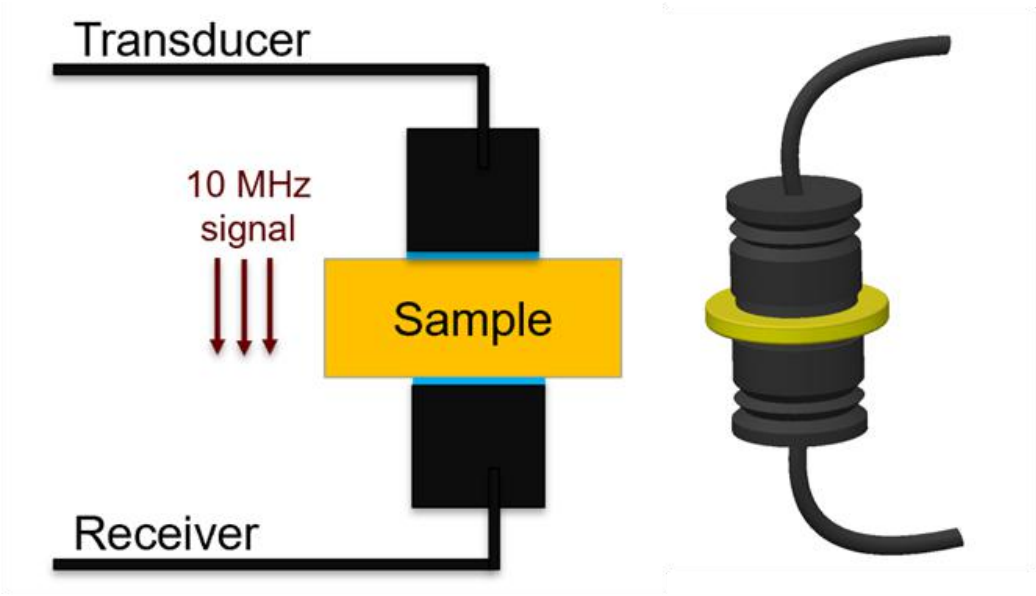

Figure 4. Illustration of resonant ultrasound experimental set up.

The characteristic time delay needed for the signal to traverse through the material relates to the elastic constant C_{IIII}. As seen in Figure 5, there is a level of correlation between the amount of rainfall and the C_{IIII} elastic constant. Yarima experienced a decrease in rainfall from October 2017 until December 2017, which translated to a decrease in elastic constant at 10 MHz. Looking at the samples from 2018, overall rainfall had an increasing trend, translating to an increase in the elastic constant. The non-destructive method of quantifying mechanical response at very short time scales revealed more considerable elasticity in a rubber sample with higher rainfall. To create a material with a reduced degree of variability between months, cultivators can log the rainfall amount present in their region and irrigate appropriately to reduce rainfall-induced variations present within the extracted latex. Agricultural labs could conduct controlled experiments where rainfall would be applied artificially to allow for a more robust proof of how rainfall influences NR's elastic behavior.

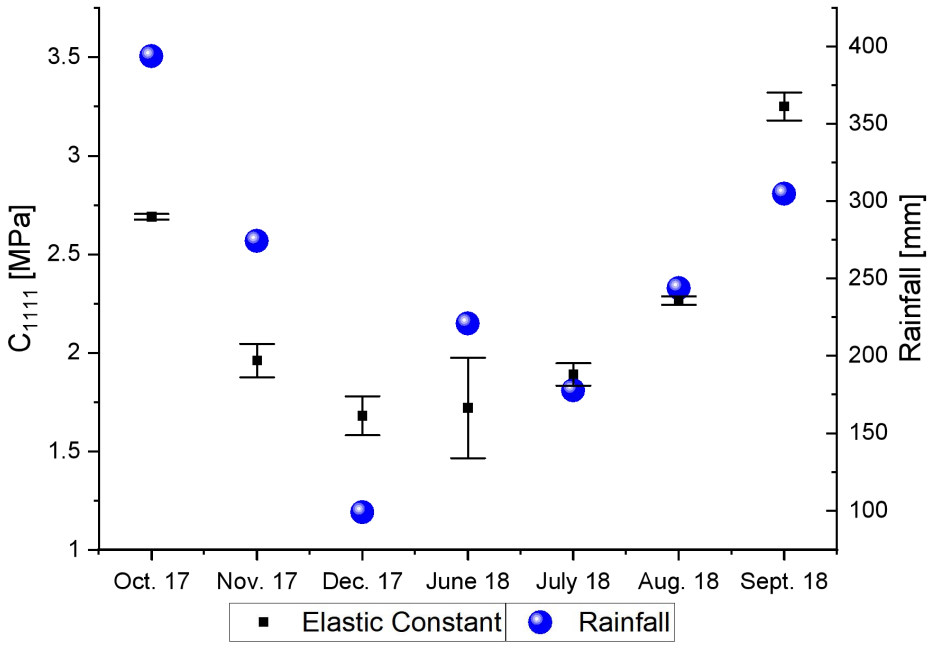

Figure 5. Graph depicting the correlation between monthly rainfall in Yarima and the C_{1111} elastic constant.

Additionally, it has been discovered that higher temperatures result in high *evapo*-transpiration rates of the rubber plant, which reduces the net accumulation of photosynthates [4]. Therefore, the living plant tissues' mechanical properties can depend upon the magnitude of turgor pressure mentioned above. A higher turgor pressure reduces the magnitude of cell wall deformation due to being in axial tension, and there is an increase in the elastic modulus of the plant tissue [26,27].

3.4. Stress relaxation studies

Relaxation measurements in tension resulted in a low degree of variability within the sample rolls and a high degree of repeatability between all five experiments per roll. Figure 6 below illustrates an overlay of relaxation experiments from various samples from distinct months, where the characteristic relaxation curve can be seen for one experimental condition. As experiments were conducted at three different temperatures, the temperature-dependent behavior was investigated to understand further the material's sensitivity to an increase in temperature.

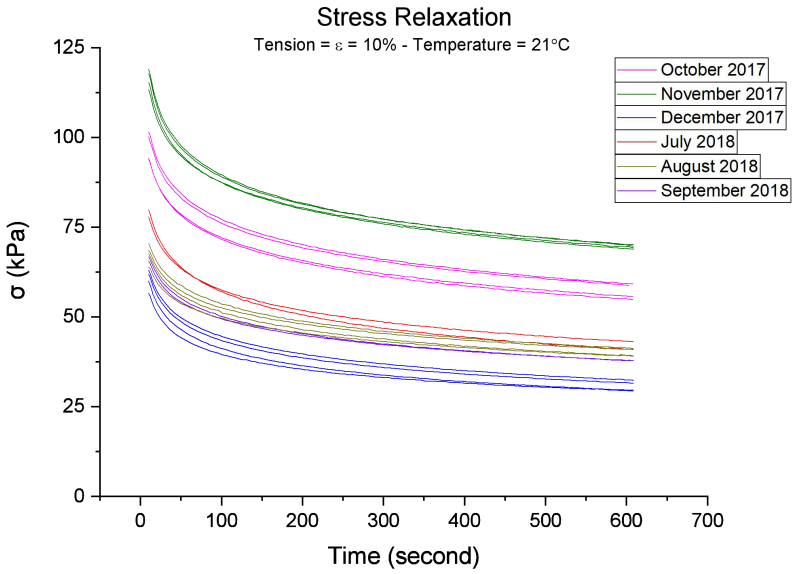

Figure 6. Tensile stress relaxation plots for various collection dates at 10% strain and 21 °C.

A temperature increase also increases the free volume within the material, improving the mobility at the molecular level of NR [28]. Higher processing temperatures translate to decreased relaxation times and decreased overall stresses experienced by the NR sample [29]. The distinctive curves can be seen overlaid in Figure 7 below, where a vertical shift is visible between each specific temperature. This vertical shift relates to the decreased necessary stress to elongate the material 10% of its original length. Furthermore, instead of analyzing one experimental condition, a more extensive analysis was needed to understand the temperature-dependent behavior of NR, and a master curve could be used to model the long-term viscoelastic response of this material.

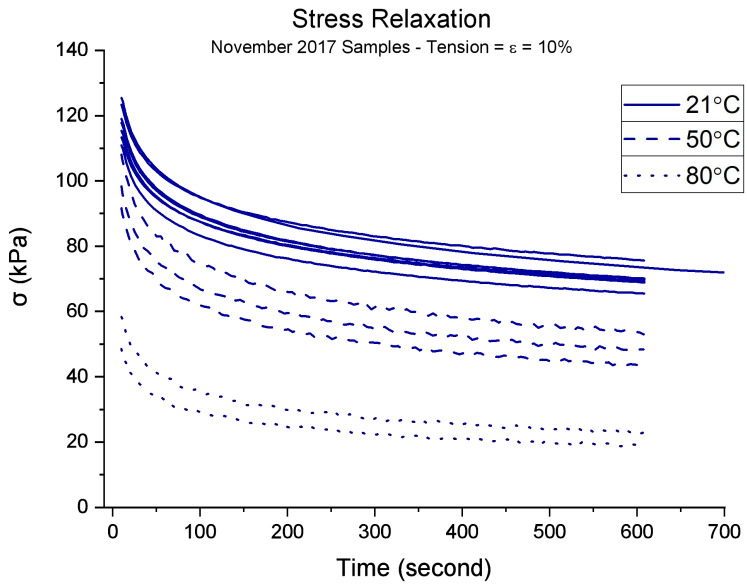

Figure 7. Stress relaxation measurements at 10% strain at 21 °C, 50 °C, and 80 °C.

As NR takes hours to relax to 1% of the maximum stress experienced in testing, a master curve may be developed using the Cross WLF equation [28,30]. Figure 8 shows the three-hour-long relaxation test conducted to validate the master curve. Moreover, by testing the material at 21 °C, 50 °C, and 80 °C, a horizontal shift factor can be calculated to create the master curve for each distinct month, as seen below in Figure 9.

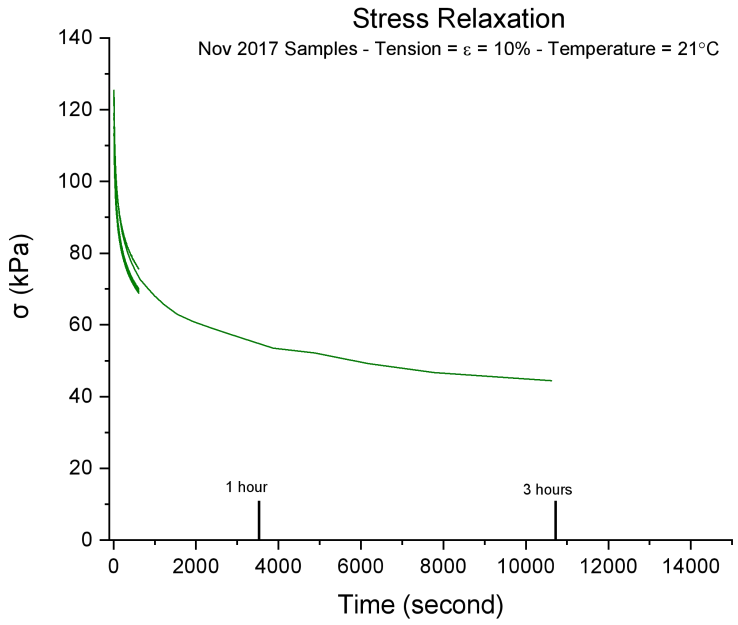

Figure 8. Plot depicting the 3-hour relaxation test used to validate the master curve.

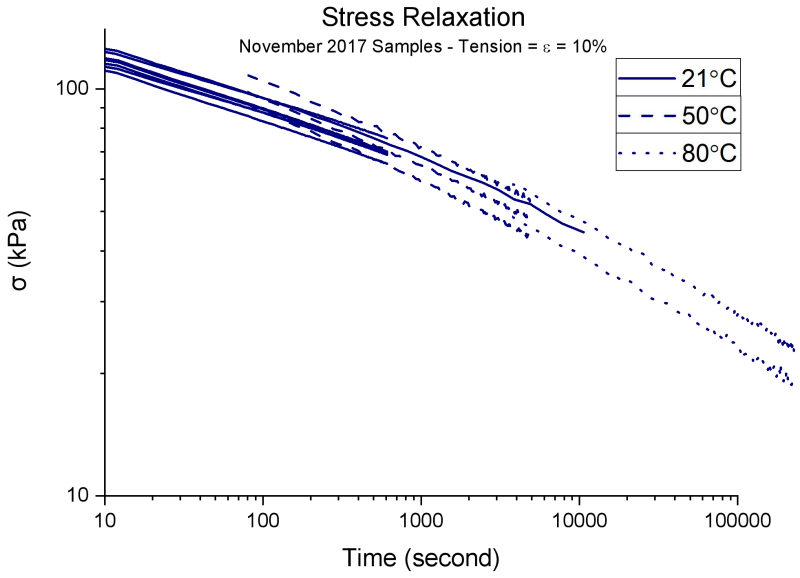

Figure 9. The stress relaxation master curve for samples from November of the year 2017 at 10% elongation.

Moreover, the relaxation measurements can be fit to a power-law [31] as seen below where the A constant relates to the starting position of the stress response, and the b constant relates to the rate at which the stress decays. The rate at which the stress decays gives an indirect method of quantifying the relaxation time, as a larger b value translates to quicker stress decay and shorter relaxation time. This simplification method eliminates the need to use the Cross WLF equation for all cases. The b constant can be determined for the three distinct temperatures for each sample and the change of b with respect to temperature ($\frac{db}{dT}$) was calculated to determine the temperature sensitivity of the material.

$$\sigma = At^b \tag{2}$$

$$\alpha = \frac{db}{dT} \tag{3}$$

Table 1 below depicts the b constant for each experiment, displaying that the magnitude of the constant increases, which relates to a quicker decay in stress. Table 2 below highlights α, the constant which was determined by $\frac{db}{dT}$, an indirect method of quantifying the sensitivity of the material as processing temperatures change. Compared to the amount of rainfall within the region in Figure 10, the magnitude of the sensitivity parameter a decreases when rainfall decreases.

Table 1. List of b constant values at differing temperatures and months of the year.

Collection month	$b_{21°C}$	$b_{50°C}$	$b_{80°C}$
October 2017	−0.13	−0.19	−0.26
November 2017	−0.13	−0.18	−0.23
December 2017	−0.17	−0.21	−0.26
June 2018	−0.12	−0.19	−0.25
July 2018	−0.16	−0.20	−0.28
August 2018	−0.13	−0.20	-
September 2018	−0.14	−0.20	−0.29

Table 2. Values for describing the sensitivity of NR related to changes in processing conditions.

Collection month	α
October 2017	−0.0021
November 2017	−0.0017
December 2017	−0.0015
June 2018	−0.0022
July 2018	−0.0020
August 2018	−0.0022
September 2018	−0.0026

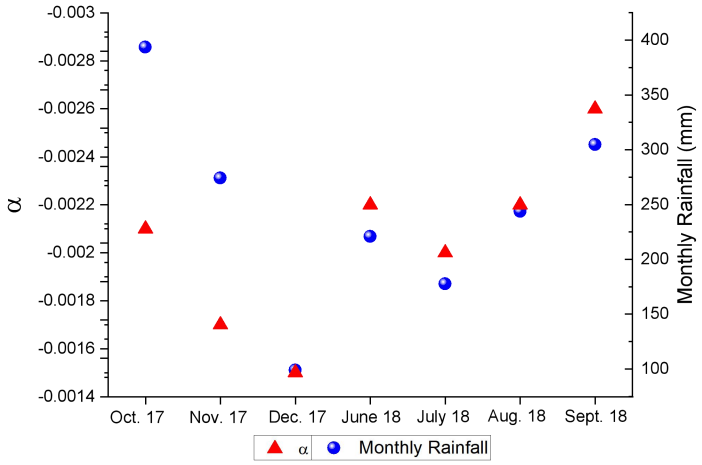

Figure 10. This plot depicts the relationship between the rainfall amount and the temperature sensitivity parameter α.

3.5. Storage-induced effects

Furthermore, understanding the storage-induced effects is vital for prolonging the shelf-life of NR. Due to NR's unstable nature, prolonged storage times may lead to the further crystallization of NR, ultimately altering the material's final performance. Although this occurrence is slow-paced and requires specific environmental conditions, it may still modify the final part performance. The material's maximum shear stress was logged for each stress relaxation measurement at various exposure times in the oxidative environment. Materials stored for a more extended period exhibit a more consistent maximum stress with increased exposure in the oxidative environment. The red curves in Figure 11 below represent the samples from the year 2017, and the black curve represents samples from the year 2018. This figure depicts how samples originating from a previous year have a lower decomposition rate when exposed to 210 °C, in air and for a prolonged time.

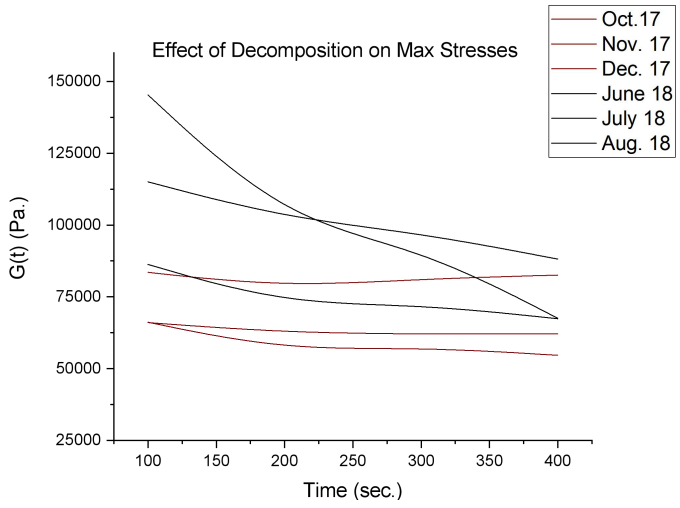

Figure 11. Graph for the influence of storage time on the decomposition rate of material when exposed at high temperatures.

Similarly, masticating the material under critical stresses causes the average molecular weight to diminish and shows an overall change in molecular weight distribution. The degradation of polymeric chains reduces the molecular weight distribution of the material, and as proven by Tzoganakis and coworkers, this shift in molecular weight distribution leads to an increase in melt index [32]. This improvement in flow is visible when placing an NR sample between parallel plates and imposing a steady shear strain input of 10% at 210 °C while exposed to nitrogen or air exclusively. Figure 12 below depicts the oxidative behavior of the NR samples when processed in air or nitrogen. The NR sample's onset temperature occurs about 30 °C sooner in the air than when processed in nitrogen, and that the overall mass decays at a greater rate compared to when processed in nitrogen.

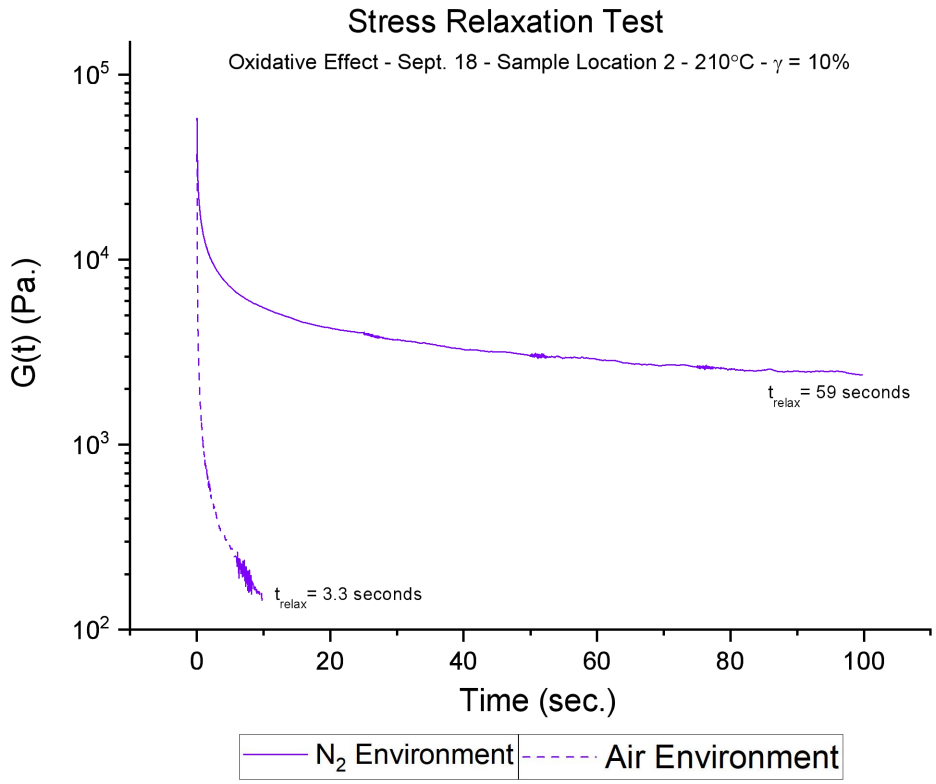

Figure 12. Stress relaxation comparison between a non-oxidative environment and an oxidative environment.

Moreover, as seen in Figure 12, the relaxation behavior changes drastically if processed in an environment that impedes degradation due to atmospheric effects. When processed in nitrogen, the relaxation time equates to 59 seconds, while it is about 3 seconds in air. This rapid decay in stress connects to the adverse effects of degradation on rheological behavior related to the thermogravimetric analysis seen in Figure 13, where onset occurs sooner when processed in air and decay occurs much rapidly afterward. The polymeric chains' thermal degradation improves the molecules' ability to align in the direction of the stress, resulting in decreased relaxation behavior, depicted in Figure 12. Although polymeric chain degradation improves the material's processability, it does so at the expense of the mechanical properties of NR that make it so desirable.

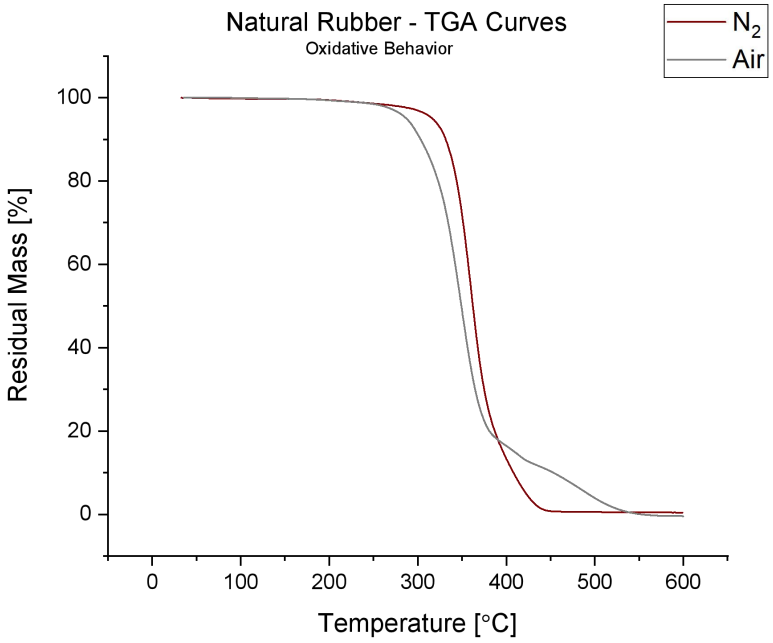

Figure 13. Thermogravimetric analysis plots showing the accelerated decomposition when the sample is exposed to an oxidative environment.

4. Conclusions

The following NR characterization study observed how climate influences NR's viscoelastic, thermal, and mechanical behavior extracted from that specific region. The elastic constant of the raw unvulcanized NR increased with increased rainfall in the region, and the amount of crystallization within the material increased with decreased rainfall. Similarly, rainfall also influenced the sensitivity of the material when exposed to varying temperatures. These climate-induced variations are vital for designing components that require stringent specifications with NR and are crucial to source material from regions where the agricultural process is optimized for consistent yield and quality. As 85% of NR's global production is provided by small plantations smaller than 5 hectares, strategies are most likely not implemented to optimize the yield and material consistency throughout the property [33]. Large-scale corn producers in the United States utilize irrigation strategies, artificial intelligence, chlorophyll measurements, and much more to optimize their yield and quality. The same strategies can be implemented in NR plantations to ensure quality and yield are consistent throughout various seasons. This change would guarantee specific properties for those interested in producing higher quality products with this sustainable elastomer.

Conflict of interest

The authors declare no conflict of interest.

Author contributions

Allen Jonathan Román: investigation, evaluation, conceptualization, and writing; Jamelah Zena Travis: investigation, evaluation, and writing; Juan Carlos Martínez Ávila: investigation; Tim A. Osswald: conceptualization.

References

1. Umar HY, Okore NE, Toryila M, et al. (2017) Evaluation of impact of climatic factors on latex yield of hevea brasiliensis. DOI: 10.20431/2454-6224.0305004.
2. Rao P and Vijayakumar KR (1992) *Natural rubber: Biology, Cultivation and Technology Development in Crop Science*, Elsevier Science.
3. Mesike CS and Esekhade TU (2014) Rainfall variability and rubber production in Nigeria. *Afr J Environ Sci Technol* 8: 54–57.
4. Kenneth OO and Okeoghene AE (2006) Evaluation of five weather characters on latex yield in hevea brasiliensis. *Int J Agr Res* 1: 234–239.
5. Craciun G, Manaila E, Stelescu MD (2016) New elastomeric materials based on natural rubber obtained by electron beam irradiation for food and pharmaceutical use. *Materials* 9: 999.
6. Osswald TA (2017) *Understanding Polymer Processing*, 1 Ed., München: Carl Hanser Verlag GmbH Publications.
7. Kuang X, Chen K, Dunn CK, et al. (2018) 3D printing of highly stretchable, shape-memory, and self-healing elastomer toward novel 4D printing. *ACS Appl Mater Interfaces* 10: 7381–7388.
8. Choi JH, Kang HJ, Jeong HY, et al. (2005) Heat aging effects on material property and the fatigue life of vulcanized natural rubber, and fatigue life prediction equations. *J Mech Sci Technol* 19: 1229–1242.
9. Martinez JRS, Le Cam JB, Balandraud X, et al. (2013) Mechanisms of deformation in crystallizable natural rubber. Part 1: thermal characterization. *Polymer* 54: 2717–2726.
10. Brüning K, Schneider K, Roth SV, et al. (2012) Kinetics of strain-induced crystallization in natural rubber studied by WAXD: dynamic and impact tensile experiments. *Macromolecules* 45: 7914–7919.
11. Wei Y, Zhang H, Wu L, et al. (2017) A review on characterization of molecular structure of natural rubber. *MOJ Poly Sci* 1: 197–199.
12. Kitaura T, Kobayashi M, Tarachiwin L, et al. (2018) Characterization of natural rubber end groups using high-sensitivity NMR. *Macromol Chem Phys* 219: 1700331.
13. Sakdapipanich JT and Rojruthai P (2012) Molecular structure of natural rubber and its characteristics based on recent evidence. In: Sammour RH, *Biotechnology-Molecular Studies and Novel Applications for Improved Quality of Human Life*, Croatia: InTech, 213.
14. Tanaka Y (2001) Structural characterization of natural polyisoprenes: Solve the mystery of natural rubber based on structural study. *Rubber Chem Technol* 74: 355–375.
15. Tanaka Y, Sato H, Kageyu A (1983) Structure and biosynthesis mechanism of natural cis-polyisoprene from Goldenrod. *Rubber Chem Technol* 56: 299–303.
16. Tangpakdee J, Tanaka Y, Ogura K, et al. (1997) Structure of in vitro synthesized rubber from fresh bottom fraction of Hevea latex. *Phytochemistry* 45: 275–281.
17. James CR (1984) *NMR and Macromolecules*, Washington: American Chemical Society.
18. Tanaka Y, Takeuchi Y, Kobayashi M, et al. (1971) Characterization of diene polymers. I. Infrared and NMR studies: nonadditive behavior of characteristic infrared bands. *J Polym Sci Pol Phys* 9: 43–57.

19. Sato H and Tanaka Y (1979) ^{1}H-NMR study of polyisoprenes. *Polym Sci: Polym Chem Ed* 17: 3551–3558.
20. Sotta P and Albouy PA (2020) Strain-induced crystallization in natural rubber: flory's theory revisited. *Macromolecules* 53: 3097–3109.
21. Lakes RS (2004) Viscoelastic measurement techniques. *Rev Sci Instrum* 75: 797–810.
22. Bruker (2014) *Bruker Avance Beginners Guide*, Bruker Corporation Publishing, 23–30.
23. Chen HY (1962) Determination of cis-1,4 and trans-1,4 contents of polyisoprenes by high resolution nuclear magnetic resonance. *Anal Chem* 34: 1793–1795.
24. Basfar AA, Abdel-Aziz MM, Mofti S (2002) Influence of different curing systems on the physico-mechanical properties and stability of SBR and NR rubbers. *Radiat Phys Chem* 63: 81–87.
25. Gooding EGB (1952) Studies in the Physiology of Latex III. Effects of Various Factors on the Concentration of Latex of Hevea brasiliensis. *New Phytol* 51: 139–153.
26. Ellis EC, Turgeon R, Spanswick RM (1992) Quantitative analysis of photosynthate unloading in developing seeds of phaseolus vulgaris L.: II. pathway and turgor sensitivity. *Plant Physiol* 99: 643–651.
27. Niklas KJ (1989) Mechanical behavior of plant tissues as inferred from the theory of pressurized cellular solids. *Am J Bot* 76: 929–937.
28. Osswald TA and Rudolph N (2015) Polymer Rheology, München: Carl Hanser Verlag GmbH Publications.
29. Minoura Y and Kamagata K (1964) Stress relaxation of raw natural rubber. *J Appl Polym Sci* 8: 1077–1087.
30. Tosaka M, Kawakami D, Senoo K, et al. (2006) Crystallization and stress relaxation in highly stretched samples of natural rubber and its synthetic analogue. *Macromolecules* 39: 5100–5105.
31. Lakes R, Lakes RS (2009) *Viscoelastic Materials*, UK: Cambridge University Press.
32. Tzoganakis C, Vlachopoulos J, Hamielec AE (1988) Production of controlled-rheology polypropylene resins by peroxide promoted degradation during extrusion. *Polym Eng Sci* 28: 170–180.
33. Wainwright-Déri E, Rubber–does 'natural' mean sustainable?, 2018. Available from: https://www.spott.org/news/rubber-does-natural-mean-sustainable/.